

ELECTROMAGNETIC AND THERMAL PHENOMENA IN THE CONTROLLED PHASE TRANSFORMATION MELTING PROCESS

Ștefan Nagy* — Mojmír Kollár**

This paper presents the electromagnetic and thermal phenomena during the melting process, with phase transformation control, of ferromagnetic alloys. The probes cast using this method will have a uniform structure, without micro-fissures. If the solid's part growth of the molten is controlled, we can stop the process that creates solidification centers, thus the material structure will be homogenous. A solution for this matter is given by the control of the solidification layer (phase transformation) using forced heating of the liquid part with eddy currents and forced cooling of the solid part. The evolution of the area with eddy currents and the cooled one, controls the phase transformation.

Key words: eddy currents, electromagnetic field, thermal field, controlled phase transformation

1 INTRODUCTION

The solidification of a melted metal starts in solidification centers, usually associated to impurities, from where it progresses gradually in the whole body. The result is a non-homogenous structure with internal stresses, which often lead to micro-fissures. A solution that offers the control over the hardening surface is to heat the liquid with eddy currents combined with a forced cooling of the hardened part. Controlling the movement of the crucible and the cooling system relative to the excitation coil, we can control the evolution of the hardening surface [1], [2] and [5].

The coupled electromagnetic and thermal fields problems are usually solved using the finite elements method [3], using the same mesh in both cases. The main drawback is that we have to adapt the mesh to the movement of the crucible in the induction coil. The method of the integrate equation of eddy currents eliminates this inconvenient, but the system matrix is full. However, the mesh is associated only to the domains with eddy currents and we have to invert the system matrix only once.

The speed of the crucible in the induction coil is sufficiently small that we can overlook the eddy currents' component due to movement, and we can admit a sinusoidal regime in the electromagnetic field problem.

In order to determine the losses we use the integral equation of eddy currents. Then we solve the thermal diffusion problem, obtaining the evolution of the solidification layer. The mesh used to determine the numeric solution of the integral equation is also used for solving the thermal diffusion problem by finite differential method or the finite elements method. The boundary conditions for the thermal problem vary in time due to the movement

of the crucible and are required at the surface of the domains with eddy currents. The thermal diffusion equation is nonlinear, due to the presence of the solidification layer. In order to illustrate the suggested procedure we developed a 2D program, but the method can also be extended to 3D structures [4].

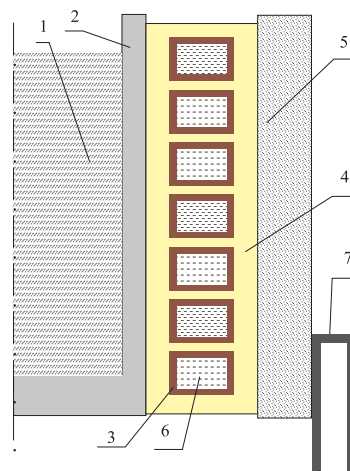


Fig. 1. The crucible and the aluminum alloy. See the text for explanation.

2 THE CRUCIBLE AND THE ALUMINUM ALLOY SAMPLE

We determine the solidification layer for a melted aluminum alloy "1" in a graphite crucible "2" (Fig. 1). The bottom of the crucible can be made out of the same material like the sidewalls, but not necessarily. Around the crucible there are the coils of the inductor "3" that induce the eddy currents and produce the Joule losses. Within the coil there is a water flow "6". The coil is separated

*University of Oradea, Faculty of Electrical Engineering and Information Technology, 1, Universitatii Street, 410087 - Oradea, Romania, E-mail: snagy@rdslink.ro

**Slovak University of Technology, Faculty of Electrical Engineering and Information Technology, Department of Electromagnetic Theory, Ilkovičova 3, 812 19 Bratislava, Slovakia, E-mail mojmir.kollar@stuba.sk

from the crucible and the yokes "5" by an isolator layer of asbestos "4". The crucible is lowered into the cooling system "7".

The crucible can move vertically, downwards, into the cooling system. This way, in the lower part of the molten it starts the solidification process. The shape of the solidification layer and its' propagation speed depend on the losses produced by the eddy currents, the speed of the crucible and the cooling conditions.

3 COMPUTATION OF EDDY CURRENTS

If the magnetic permeability of the environment is μ , then the contribution of an infinitely small piece of a conductor (with cross section dS and length dr) to the magnetic potential vector produced by its current is

$$d\vec{A}(\vec{R}) = \frac{\mu}{4\pi} \frac{\vec{J}(\vec{r})dV}{|\vec{R} - \vec{r}|} \quad (1)$$

where $dV = dSdr$ and \vec{R} and \vec{r} are the position vectors of the investigated point and source (a piece of the conductor) respectively, see Fig. 2.

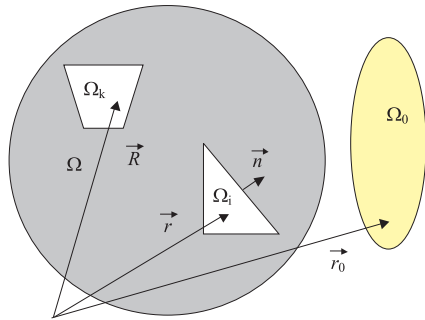


Fig. 2. To development of electromagnetic field equations to be solved numerically.

Consider Ω_0 to be the domain with a given current density $\vec{J}_0 = \vec{k}_0 J_0$ and Ω to be the domain crossed by the eddy currents with the density $\vec{J} = \vec{k} J$. We assume that in Ω_0 we have a completely defined current system. The magnetic potential vector due to these two current densities is

$$\vec{A}(\vec{R}) = \vec{A}_0(\vec{R}) + \frac{\mu}{4\pi} \iiint_{\Omega} \frac{\vec{J}(\vec{r})}{|\vec{R} - \vec{r}|} dV \quad (2)$$

where

$$\vec{A}_0(\vec{R}) = \frac{\mu}{4\pi} \iiint_{\Omega_0} \frac{\vec{J}(\vec{r})}{|\vec{R} - \vec{r}_0|} dV \quad (3)$$

From the law of electromagnetic induction we have

$$\text{rot } \vec{E} = -\frac{\partial \vec{B}}{\partial t} = -\frac{\partial}{\partial t} \text{rot } \vec{A} = \text{rot} \left(-\frac{\partial \vec{A}}{\partial t} \right)$$

giving

$$\vec{E} = -\frac{\partial \vec{A}}{\partial t} + \text{grad } \psi$$

In absence of the so called *free* charges, $\text{grad } \psi = 0$, and taking into consideration the conduction law one can write $\vec{J} = -\sigma \frac{\partial \vec{A}}{\partial t}$ to obtain, for in time slowly enough varying fields, after substituting from (2)

$$-\frac{\vec{J}(\vec{R}, t)}{\sigma} = \frac{\partial \vec{A}_0(\vec{R}, t)}{\partial t} + \frac{\mu}{4\pi} \iiint_{\Omega} \frac{\partial \vec{J}(\vec{r}, t)}{\partial t} \frac{dV}{|\vec{R} - \vec{r}|} \quad (4)$$

This is an integral equation for the unknown space and time dependence of current density $\vec{J}(\vec{R}, t)$. Since this paper deals with aluminum alloys, the environment is assumed to be homogenous and linear with constant permeability μ and for simplicity also with a constant conductivity σ .

In case of sinusoidal duty cycle, using the complex representation, after a short manipulation (4) becomes

$$j\delta^2 \vec{J}(\vec{R}) = \frac{2}{\mu} \vec{A}_0(\vec{R}) + \frac{1}{2\pi} \iiint_{\Omega} \frac{\vec{J}(\vec{r})}{|\vec{R} - \vec{r}|} dV \quad (5)$$

where the so called penetration depth $\delta = \sqrt{(2/\omega\mu\sigma)}$ and where

$$\frac{2}{\mu} \vec{A}_0(\vec{R}) = \frac{1}{2\pi} \iiint_{\Omega_0} \frac{\vec{J}(\vec{r})}{|\vec{R} - \vec{r}_0|} dV \quad (6)$$

Obviously

$$\begin{aligned} \vec{J}(\vec{R}, t) &= \text{Re}\{\vec{J}(\vec{R})e^{j\omega t}\} \quad \text{hence} \quad \text{Re}\{\vec{J}(\vec{R})\} = \vec{J}(\vec{R}, 0) \\ \vec{J}(\vec{A}, t) &= \text{Re}\{\vec{J}(\vec{A})e^{j\omega t}\} \quad \text{hence} \quad \text{Re}\{\vec{A}(\vec{R})\} = \vec{A}(\vec{R}, 0) \end{aligned}$$

Let domain Ω be divided into N sub-domains Ω_i in which we assume the current density to be constant, then (5) becomes

$$j\delta^2 \vec{J}(\vec{r}_k) = \frac{2}{\mu} \vec{A}_0(\vec{r}_k) + \frac{1}{2\pi} \sum_{i=1, i \neq k}^N \frac{\vec{J}(\vec{r}_i)}{|\vec{r}_k - \vec{r}_i|} \Delta V_i \quad (7)$$

where all position vectors are now denoted as r_k, r_i , respectively. To avoid the singularity when point \vec{R} is in sub-domain Ω_i , we provide $i \neq k$ for $i, k = 1, 2, \dots, N$

Using simplified notation $\vec{J}(\vec{r}_k) = \vec{J}_k$, $\vec{J}(\vec{r}_i) = \vec{J}_i$ and $\vec{J}(\vec{r}_{0s}) = \vec{J}_{0s}$ where $s = 1, 2, \dots, S$ as far as domain Ω_0 consists of S sub-domains

$$\vec{J}_k + \lambda \sum_{i=1, i \neq k}^N a_{ki} \vec{J}_i = \vec{J}_{0k} \quad (8)$$

where $a_{ki} = \Delta V_i / |\vec{r}_k - \vec{r}_i|$ providing $k \neq i$, $\lambda = j/(2\pi\delta^2)$ and

$$\vec{J}_{0k} = -\lambda \sum_{s=1}^S \frac{\vec{J}_{0s}}{|\vec{r}_k - \vec{r}_{0s}|} \Delta V_{0s}. \quad (9)$$

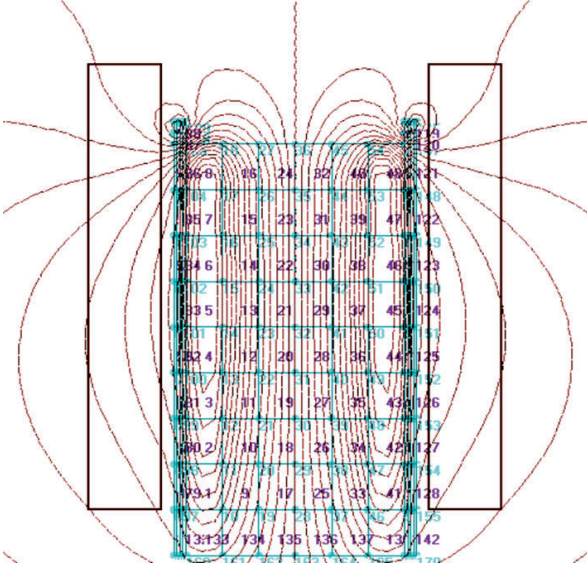


Fig. 3. The magnetic field lines at the beginning of the heating, further referred to as position 2.

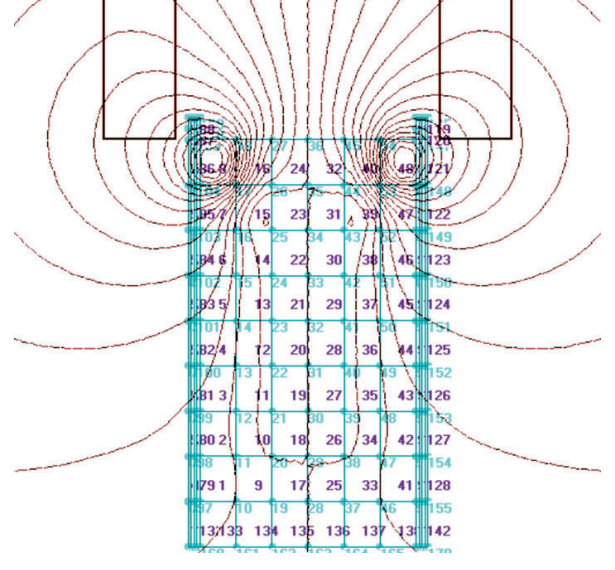


Fig. 4. The magnetic field lines at the end of the heating, further referred to as position 9.

Here, the summation is done through all values of s since always $\vec{r}_k \neq \vec{r}_{0s}$. May the current density \vec{J}_0 in Ω_0 be distributed evenly $\vec{J}_0 = \text{constant}$, the last formula will simplify accordingly.

For an axisymmetrical case the last may be modified introducing M adjacent arc elements of appropriate length l_m along the circumference. Using notation $\vec{J}(\vec{r}_{kn}) = \vec{J}_{kn}$, $\vec{J}(\vec{r}_{im}) = \vec{J}_{im}$, $\vec{J}(\vec{r}_{0sm}) = \vec{J}_{0sm}$ where $n, m = 1, 2, \dots, M$

$$\vec{J}_{kn} + \lambda \sum_{i=1}^N \sum_{m=1}^M a_{knim} \vec{J}_{im} = \vec{J}_{0kn} \quad (10)$$

where $a_{knim} = \Delta S_i l_{im} / |\vec{r}_{kn} - \vec{r}_{im}|$ providing $kn \neq im$, and as before $\lambda = j / (2\pi\delta^2)$ and

$$\vec{J}_{0kn} = -\lambda \sum_{s=1}^S \Delta S_{0s} \sum_{m=1}^M \frac{l_{sm}}{|\vec{r}_{kn} - \vec{r}_{0sm}|} \vec{J}_{0sm}. \quad (11)$$

Note that the length of individual arcs l_{im} , and/or l_{sm} in some instances may be not a constant but rather dependent on radius in cylindrical co-ordinate system which will be different for individual sub-domains ("i-th" in Ω , "s-th" in Ω_0). On the other hand, since there is no apparent reason for the consecutive arcs (at a given radius in cylindrical co-ordinate system) be of different length, index m at these can be omitted leaving thus l_i and l_s as useful parameters.

To make the solution simpler we shall now suppose the structure in Fig. 1 is a 2D because of being of: (i) a finite and small l , or (ii) infinite length l in direction perpendicular to the plane shown in figure. In either case $\Delta V = l \Delta S$. Effectively one can account for a change of length l by a change of parameter λ like follows: $\Delta V_i = l \Delta S_i$, $\Delta V_{0s} = l \Delta S_{0s}$ and let us denote $a_{ki} = l a'_{ki}$

and $\lambda' = l \lambda = j l / (2\pi\delta^2)$. From above equations for $n = 1$ and $m = 1$, in a case of homogenous current density distribution in the coils of inductor ("3" in Fig. 1), one gets

$$\mathcal{J}_k + \lambda' \sum_{i=1, i \neq k}^N a'_{ki} \mathcal{J}_i = -\lambda' a_{k0} \mathcal{J}_0$$

where

$$a'_{ki} = \Delta S_i / |\vec{r}_k - \vec{r}_i| \quad (12)$$

$$a_{k0} = \sum_{s=1}^S \frac{\Delta S_{0s}}{|\vec{r}_k - \vec{r}_{0s}|}.$$

To conclude: a'_{ki} and a_{k0} are evaluated once a mesh is chosen, \mathcal{J}_0 is constant and λ' depends on the (effective) length l of the discussed structure. After solving the above system of equations for the current density phasors \mathcal{J}_k , in the original set of subdomains ($k, i \in 0, N$) one can find the phasors of vector potential \mathcal{A}_p in individual subdomains of new, and even a finer, grid ($p, i \in 0, P$) using

$$\mathcal{A}_p = \frac{\mu l}{4\pi} \left\{ a_{p0} \mathcal{J}_0 + \sum_{i=1, i \neq p}^P a'_{pi} \mathcal{J}_i \right\} \quad (13)$$

and eventually, use a discrete version of $\vec{B} = \text{rot } \vec{A}$. Here, depending only on changes $\Delta x, \Delta y$ of two mutually perpendicular in-plane coordinates – the magnetic induction lines are

$$\mathcal{H}_{px} = \frac{1}{\mu} \frac{\Delta \mathcal{A}_p}{\Delta y} \quad \mathcal{H}_{py} = -\frac{1}{\mu} \frac{\Delta \mathcal{A}_p}{\Delta x} \quad (14)$$

Figures 3 and 4 show the magnetic field lines in an intermediate position of the crucible for a deliberately chosen small angle $\omega t = 4$ deg. In Fig. 5 to Fig. 6 are given variations of current density phasors and the dissipated power across the crucible at two different positions 2 and 9, of the crucible (compare Fig. 11).

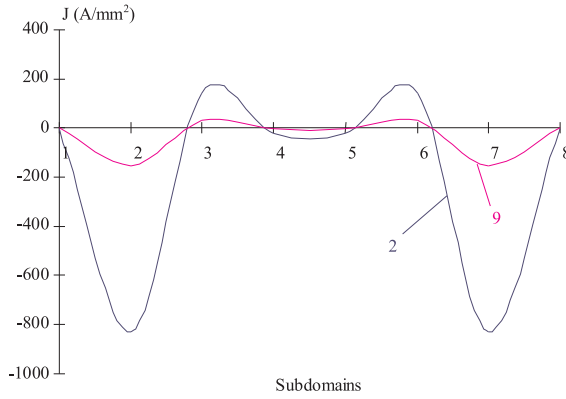


Fig. 5. Variation of imaginary part of \mathcal{J}_k across the crucible at two different positions 2 and 9, ie at the beginning and after the heating.

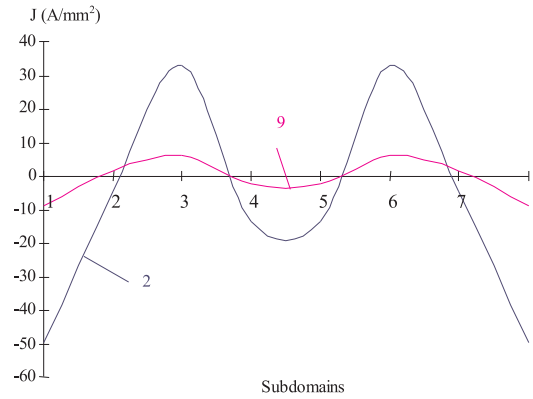


Fig. 6. Variation of real part of J_k across the crucible at different positions 2 and 9, ie at the beginning and after the heating.

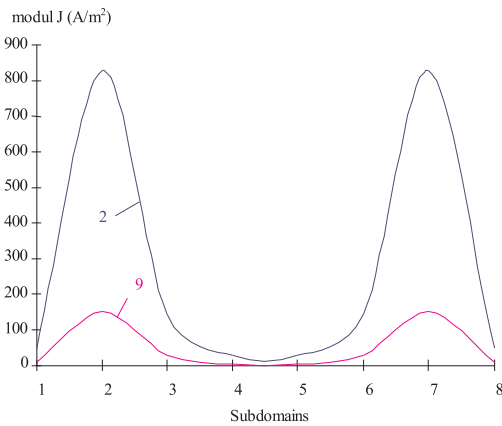


Fig. 7. Variation of J module across the crucible at at different positions 2 and 9, ie at the beginning and after the heating.

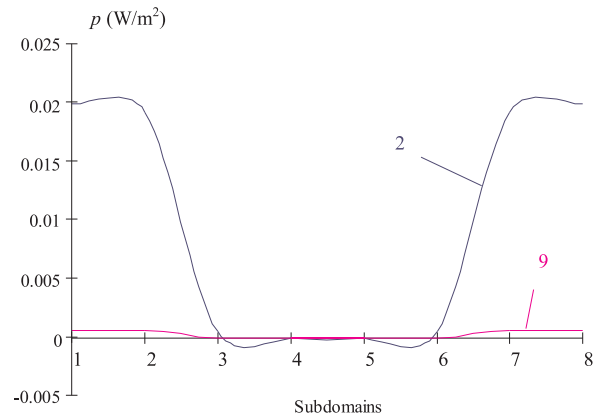


Fig. 8. Variation of volume density of the dissipated active power across the crucible at different positions 2 and 9, ie at the beginning and after the heating.

4 COMPUTATION OF THE THERMAL FIELD

We have to solve a non-linear problem with temperature dependent caloric capacity $c(T)$. The best numeric procedures are the differential ones, and given the geometry of the piece, we chose the finite differential method with advantageous polyhedral domains. The equation of the thermal field diffusion is

$$\operatorname{div}(k \operatorname{grad} T) + c(T) \frac{\partial T}{\partial t} = p \quad (15)$$

with the boundary conditions

$$-k \frac{\partial T}{\partial n} = \alpha(T - T_{ex}) \quad (16)$$

where, k – is the thermal conductivity, p – is the density of dissipated power and, caloric capacity $c(T)$ abruptly changes (specified further) when the phase shift occurs. According to Fig. 9. in points from O_1 to O_4 the term $k \operatorname{grad} T$ can be estimated to have components

$$\begin{aligned} O_1 : \frac{k_1}{h} \begin{pmatrix} T_1 - T_0 \\ T_2 - T_0 \end{pmatrix}, O_2 : \frac{k_2}{h} \begin{pmatrix} T_0 - T_3 \\ T_2 - T_0 \end{pmatrix} \\ O_3 : \frac{k_3}{h} \begin{pmatrix} T_0 - T_3 \\ T_0 - T_4 \end{pmatrix}, O_4 : \frac{k_4}{h} \begin{pmatrix} T_1 - T_0 \\ T_0 - T_4 \end{pmatrix} \end{aligned} \quad (17)$$

where $T_\nu = T(P_\nu), \nu = 0, 1, \dots, 4$ and for the sake of simplicity we chose $h = \Delta x, h = \Delta y$. For a discrete variant of the *divergence* assigned to point P_0 , we can use the mean (average) of appropriate terms in points O_1, O_4 and O_2, O_3 for Δx and O_1, O_2 and O_3, O_4 for Δy , eventually to get after a short manipulation for the square O_1, O_2, O_3, O_4, O_1 (area h^2 , shaded in Fig. 9)

$$a_{00}T_0 + a_{01}T_1 + a_{02}T_2 + a_{03}T_3 + a_{04}T_4 + b_0 \frac{\partial T}{\partial t} \Big|_{T_0} = d_0 \quad (18)$$

where

$$\begin{bmatrix} a_{00} \\ a_{01} \\ a_{02} \\ a_{03} \\ a_{04} \\ b_0 \\ d_0 \end{bmatrix} = \begin{bmatrix} -k_1 - k_2 - k_3 - k_4 \\ \frac{1}{2}(k_1 + k_4) \\ \frac{1}{2}(k_2 + k_3) \\ \frac{1}{2}(k_1 + k_2) \\ \frac{1}{2}(k_3 + k_4) \\ \frac{h^2}{4}(c_1 + c_2 + c_3 + c_4) \\ \frac{h^2}{2}(p_1 + p_2 + p_3 + p_4) \end{bmatrix} \quad (19)$$

and where d_0 varies in time and is given by the losses computed by the "electromagnetic" program. The most difficult part in solving the equation systems like (17)

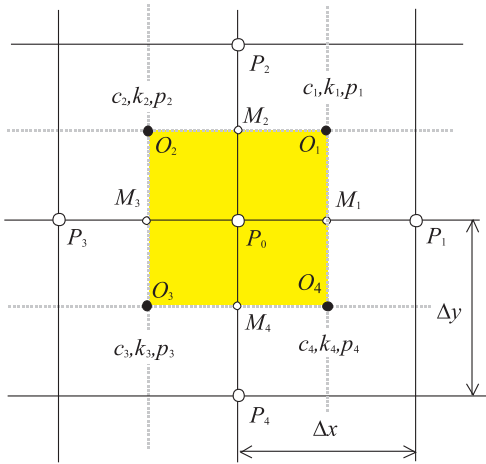


Fig. 9. To evaluation of discrete approximations of "grad" and "div" operators to be used for solving equations (15) and (16).

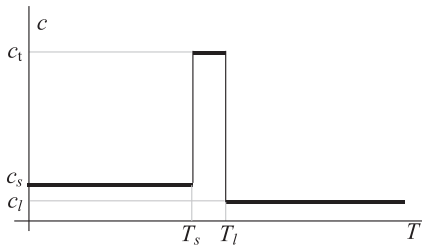


Fig. 10. Step-wise modelling of the dependency of caloric capacity at a solid-melt transition taking into account the melting latent heat.

comes from the non-linearity introduced by parameter b_0 that depends on the temperature. For simplicity we may consider a step-by-step variation of the caloric capacity (Fig. 10).

In figure 10 T_l and T_s are the temperatures that delimit the phase variation zone, and c_l , c_s and c_t are the thermal capacities of the liquid and solid alloy and in the solidification zone. T_s , T_l and c_t are chosen so that $T_{sl} = (T_s + T_l)/2$ and $c_t(T_l - T_s) = Q$, where T_{sl} is the solidification temperature and Q is latent heat of melting.

In order to numerically integral equation (18) we chose a Crank-Nicholson procedure with a coefficient of 0.5 (the trapezoidal rule).

$$\begin{aligned} & (a_{00}T'_0 + a_{01}T'_1 + a_{02}T'_2 + a_{03}T'_3 + a_{04}T'_4) \frac{\Delta t}{2} + \\ & (a_{00}T_0 + a_{01}T_1 + a_{02}T_2 + a_{03}T_3 + a_{04}T_4) \frac{\Delta t}{2} + \\ & u(T'_0)(T'_0 - T_0) = c'_0 \frac{\Delta t}{2} + c_0 \frac{\Delta t}{2} \end{aligned} \quad (20)$$

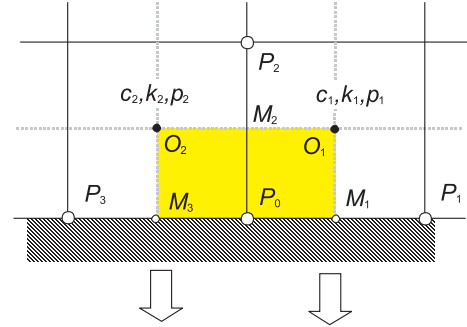
where T' are unknown temperatures at $t + \Delta t$, while T are the known temperatures at t .

The coefficient $u(T'_0)$ is computed iteratively depending on T'_0 . For example, if $T_0, T'_0 > T_l$, then $u(T'_0) = b_{0l}(T'_0 - T_0)$, while if $T_s < T'_0 < T_l < T_0$, then $u(T'_0) =$

$b_{0l}(T_l - T_0) + b_{0t}(T'_0 - T_l)$, where b_{0l} and b_{0t} contain capacities in liquid and solidification zone, respectively.

The time step Δt has to be so small that the iterative numeric procedure will be stable.

If P_0 is on the boundary, using the following scheme



$$k_3 \frac{\partial T}{\partial n} = -\alpha_3(T - T_{ex3}) \quad k_1 \frac{\partial T}{\partial n} = -\alpha_1(T - T_{ex1})$$

one can find the finite differential equation (18) be altered to

$$a'_{00}T_0 + a'_{01}T_1 + a'_{02}T_2 + a'_{03}T_3 + b'_0 \frac{\partial T}{\partial t} \Big|_{T_0} = d'_0 \quad (21)$$

where

$$\begin{bmatrix} a'_{00} \\ a'_{01} \\ a'_{02} \\ a'_{03} \\ b'_0 \\ d'_0 \end{bmatrix} = \begin{bmatrix} -k_1 - k_2 \\ k_1 - h\alpha_1 \\ k_1 + k_2 \\ k_2 - h\alpha_3 \\ \frac{h^2}{2}(c_1 + c_2) \\ \frac{h^2}{2}(p_1 + p_2) - h(\alpha_1 T_{ex1} + \alpha_3 T_{ex3}) \end{bmatrix} \quad (22)$$

The boundary conditions vary in time along with the position of the crucible, because under the inductor is the cooling system. Thus, the external temperature T_{ex} and coefficients α are modified at every time step.

The software program, developed at University of Oradea, allows to graphically visualize isotherms at any moment during the process when the solidification layer is in motion. To solve the electromagnetic problem the software package consists of 9 programs. From them 1 to 6 are run first and then for each time-step are running programs 7, 8 and 9. The system allows to choose a number of steps at the beginning of the simulation. In this paper we have presented a simulation with 10 steps. To solve the thermal field another software package was developed to define the boundaries, boundary types, the boundary conditions (varying or fixed), to build up the constant part (which does not vary in time) of the system matrix and to build up the time-varying part of the system matrix proceed in solving iteratively (step-by-step). Running of these program enables one to obtain the isotherms at any instant of time including that when the transition in the solidification layer occurs.

Figures 11 a) and b) present values of the alloys' temperature in the crucible at the beginning and the end of the controlled solidification process.

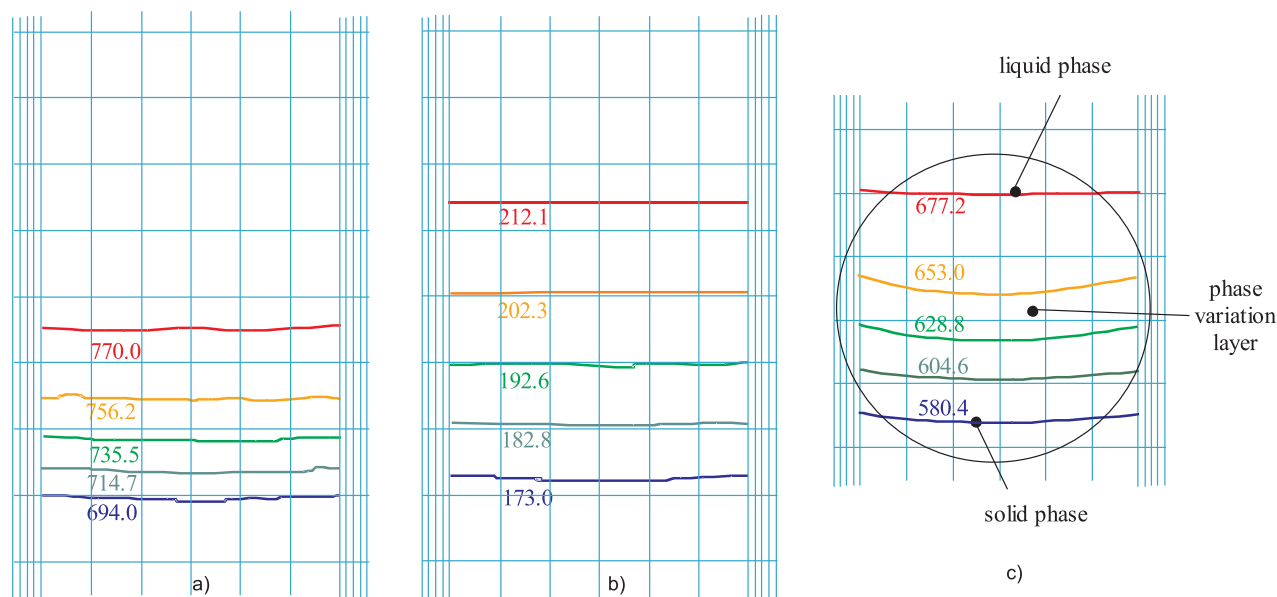


Fig. 11. Isotherms at two different positions of the crucible: a) and b) show the values of alloy temperature in the crucible at two different instants of the phase-variation-layer movement, see c) for more detailed explanation.

6 CONCLUSION

This paper presents a procedure to solve the coupled electromagnetic and thermal field problem in the casting systems techniques: solidification with controlled phase variation layer. A solution to this problem is the control of the solidification layer by forced heating of the molten using eddy currents and forced cooling of the solid part. The shape and deployment speed of the phase variation layer depend on the losses produced by the eddy currents, the speed of the crucible and the cooling conditions. In order to determine the eddy currents we use the integral equation method of the current density in a developed own software package to solve the problem. In order to solve the thermal diffusion problem we have chosen the finite difference method because of certain advantages. The same mesh can be used for both eddy currents problem and also for the thermal field problem. The data transfer about the volume density of the Joule losses between the two programs are convenient; we can easily take into account the varying boundary conditions due to the movement of crucible. We developed an iterative numerical procedure that takes into account the phase variation interval in which the thermal capacity of the molten increases very much. The suggested procedure can be extended to 3D structures [4].

REFERENCES

- [1] NAGY, S.: Aspects of electromagnetic and thermal phenomena during the process using induction ovens, Proceedings of International Conference EMES'01, Oradea (May 2001), 270-274.
- [2] MAGHIAR, T.—LEUCA, T.—HANTILA, F. I.: Numerical analysis of eddy current heating, Editura Universitatii din Oradea, Oradea, 2001. (in Romanian)
- [3] BIRO, O.—PREIS, K.: Finite element analysis of eddy currents, IEEE Trans. on Magn. No. 2 (1990), 414-423.
- [4] ALBANESE, R.—HANTILA, F. I.—PREDA, G.—RUBINACCI, G.: A nonlinear eddy current integral formulation for moving bodies, IEEE Trans. on Magn. No. 2 (1998), 2529-2534.
- [5] MAGHIAR, T.—NAGY, S.—HANTILA, I. F.—NAGY, A.: The evolution of the hardening surface in the controlled casting process, The 10th International IGTE Symposium on Numerical Field Calculation in Electrical Engineering, 16-18 sept. 2002, Graz-Austria, pp. 290-294.

Received 2 September 2004

Revised 15 November 2005

Stefan Nagy (Prof, Ing, PhD) was born in a mining town with strong industry. He graduated the Faculty of Electrical Engineering at the University of Oradea. He gained his PhD in Electrical Engineering. He designed more melting and casting equipment in various factories in Oradea. At present he teaches at the Electrical Engineering Department at the Faculty of Electrical Engineering and Information Science at the University of Oradea. His main fields of research and teaching activities are the modelling and simulation of coupled thermal and electromagnetic phenomena, and electrical technologies.

Mojmír Kollár (Ing, PhD), born in Ružomberok, Slovakia, in 1945, graduated from the Faculty of Electrical Engineering, Slovak Technical University, Bratislava, in solid state physics, in 1968. He received the PhD degree in Theory of Electromagnetism from the same university, in 1985, where he at present works as lecturer at the Department of Electromagnetic Theory. The main fields of his research and teaching activities are the circuit and electromagnetic field theory with a particular involvement in ferromagnetics.